Clays and Clay Minerals, Vol. 35, No. 5, 321–335, 1987.

COMPOSITIONAL AND STRUCTURAL VARIATIONS IN THE SIZE FRACTIONS OF A SEDIMENTARY AND A HYDROTHERMAL KAOLIN

GIANNI LOMBARDI

Dipartimento di Scienze della Terra, Università degli Studi di Roma "La Sapienza"
00185 Roma, Italy

JAMES D. RUSSELL

The Macaulay Institute for Soil Research, Craigiebuckler
Aberdeen AB9 2QJ, United Kingdom

WALTER D. KELLER

Department of Geology, University of Missouri–Columbia
Columbia, Missouri 65211

Abstract—The 16–8-, 8–5-, 5–2-, 2–1-, 1–0.5-, 0.5–0.3-, 0.3–0.1-, and <0.1-μm size fractions were centrifuged from a Georgia (U.S.A.) sedimentary kaolin and a hydrothermal kaolin from the Sasso mine (Italy) and analyzed by scanning electron microscopy (SEM), X-ray powder diffraction (XRD), infrared spectroscopy (IR), differential thermal analysis (DTA) and thermogravimetry (TGA) together with the corresponding whole rocks. All size fractions of the Georgia sample consisted dominantly of well-crystallized, fine-grained kaolinite, associated with minor quantities of smectite. Some halloysite-like elongate particles were noted by SEM in the intermediate size fractions, minor amounts of quartz were identified in the coarsest size fractions, and <1% noncrystalline material and traces of organic material were suspected in the finest size fraction. The crystallinity of the kaolinite as measured by XRD and IR varied moderately with size. IR suggested that nacrite-like stacking disorder increased with decreasing size for particles <5 μm in size.

In the Sasso sample kaolinite dominated all size fractions and was accompanied by dickite in the coarse and by halloysite in the fine size fractions. Regular mixed-layer illite/smectite (I/S) was present in all size fractions and dominated in the finest. Abundant quartz and traces of alunite were identified in the whole rock and coarsest size fractions. The kaolinite in this sample showed marked variation in stacking order and crystallinity, as shown by changes in XRD, IR, and DTA patterns.

The observed compositional and structural variations in the size fractions of the Georgia sedimentary kaolin are small, as expected from formational environment, which was characterized by low temperatures and relative stable genetic conditions. The much more marked differences in composition within the size fractions of the Sasso hydrothermal kaolin are likely a result of the broad range of temperatures and fluid chemistry of its formational environment. The sequence dickite-well-crystallized kaolinite-kaolinite-halloysite is probably temperature-dependent.

Key Words—Dickite, Halloysite, Infrared spectroscopy, Kaolinite, Particle size, Thermal analysis, Scanning electron microscopy, X-ray powder diffraction.

INTRODUCTION

Most clays are formed in environments characterized by the presence and movement of large quantities of fluids. The amount and physicochemical properties of these fluids may vary widely during the life of the multiphase systems which govern the formation of most clay mineral assemblages. Due to the fine particle size of the clays, the differences in nucleation and growth energy of the species, and the variability in duration, strength, and location of the genetic phases, different microenvironments may concentrate different minerals. These microenvironments are often characterized by different particle-size ranges.

In clay studies, specific size fractions (20–2 and <2 μm) are commonly separated to assess sample composition. Very fine size fractions are typically enriched in and more clearly display, for example, mixed-layer minerals, smectites, and noncrystalline phases. Clay studies have not, however, addressed why mineralogy and structural types vary with particle size (as, e.g., in the kaolins described by Olivier and Sennett, 1972; Galan *et al.*, 1977; Kocsardy and Heydemann, 1980; and Hassanipak and Eslinger, 1985). Experimental data from a whole rock or a <2-μm size fraction may refer to the dominant component only and mask the existence of substantial quantities of other mineralogical or structural phases. For example, Brindley *et al.* (1963) and Keller and Haenni (1978) showed that for mi-

crometer-size mixtures of kaolin minerals large amounts of a specific polymorph would not be detected on X-ray powder diffraction (XRD) traces because of the masking effect of a dominant mineral or one whose XRD reflections overprinted those of other phases.

In the present work, a systematic investigation by XRD, scanning electron microscopy (SEM), infrared spectroscopy (IR), differential thermal analysis (DTA), and thermogravimetry (TGA) was carried out on a sedimentary and a hydrothermal kaolin in order to define the variations in composition and crystallinity of the phases within their several size fractions. The analysis of the whole rock and related size fractions by different techniques gave a detailed picture of the texture, mineralogy, and structural characteristics of the single species. On the basis of SEM, XRD, IR, DTA and TGA data an attempt was made to define the sequence of events which led to the composition of the final mineral assemblages in these two genetically different types of kaolin deposits.

SAMPLES AND EXPERIMENTAL

Two types of kaolins were studied: (1) a Cretaceous, sedimentary kaolin from the McNeal-Bloodworth mine in Wilkinson County, Georgia, U.S.A. (Kaolin 915 Regular, from the Georgia Kaolin Company); and (2) a hydrothermal kaolin from the Monte Sughereto-Sasso mine (Cerveteri, Latium, Italy), which was formed by the alteration of Plio-Pleistocene acidic volcanics. Field and other data for the Georgia sample may be found in Hinckley (1965), Murray (1976), Keller (1977), Hurst (1979), and Hassanipak and Eslinger (1985); for the Sasso sample, in Keller *et al.* (1977), Lombardi and Sheppard (1977), Lombardi and Mattias (1979), and Mattias and Caneva (1979).

Size fractionation was carried out on 300 g of sample. The material was disaggregated with a rubber hammer and wet sieved, and the <44-μm size fraction was mixed for 20 min with 200 ml of distilled water in a shaker and for 10 min in a blender. An 8–10% (wt./vol.) aqueous suspension was centrifuged as many as 20 times for appropriate times and speeds (Tanner and Jackson, 1947) to obtain eight size fractions: 16–8, 8–5, 5–2, 2–1, 1–0.5, 0.5–0.3, 0.3–0.1, and <0.1 μm. The fractions were then dried at 40°–50°C. The size separates are described below as equivalent spherical diameter (e.s.d.) homogeneous fractions; therefore, due to the hydrodynamic behavior of kaolin plates and elongate halloysite particles, the separates have only a nominal relation to the indicated size ranges.

XRD was carried out on a Philips diffractometer using oriented mounts on glass slides and random mounts prepared according to the method of Byström-Asklund (1966). SEM studies were carried out on specimens newly broken to expose fresh, natural fracture surfaces. The specimens were not chemically etched or ground, thereby avoiding possible artifacts. The surfaces were lightly sputtered with a thin film of gold to carry away any excess charge from the electron beam. Energy dispersive X-ray spectra (EDX) were obtained when necessary to confirm the identification of materials. IR spectra of clay fractions (1 mg), incorporated in 170-mg, 12-mm diameter KBr disks, were recorded over the range 4000–240 cm^{-1} on a Perkin-Elmer 580B spectrometer. The spectra were obtained at room temperature or after heating the sample at 150°C for 16 hr to remove adsorbed water. A Perkin-Elmer DTA 1700 and a Stanton Redcroft Simultaneous Thermoanalyzer STA 783 were used for DTA and TGA work, respectively.

OBSERVATIONS FROM SCANNING ELECTRON MICROGRAPHS

SEM studies of the size fractions showed that the e.s.d. size assignments were in good agreement with the observed sizes of the separate aggregates and crystallites, if platy habits are considered. In contrast, particles having an elongate tubular form were as much as three times larger than the e.s.d. obtained from physical laws that are valid for spherical bodies. This discrepancy is possibly due to the fact that elongate particles have a hollow center and therefore are lighter in weight than equivalent-size platy crystals.

In the Georgia kaolin sample, SEM observations on fracture surfaces of the whole rock showed that stacks and aggregates of kaolinite were the only immediately obvious visible components of the sample. Cleavage steps occurred about every 0.05–1 μm along the stacks, which represent compact crystals. Among the stacks were spaces in which well-developed individual kaolinite crystals were randomly dispersed in the form of relatively porous aggregates. This texture may be inherited from the parent rock and/or a possible secondary crystal growth. The coarse stacks of plates occurred within a matrix of much finer flakes or clay. Although visual assessments were not quantitative, the natural size distribution of this clay (Figure 1A) appeared to be more-or-less bimodal, and the clay consisted of coarse stacks and fine particles, with intermediate sizes occurring in relatively smaller amounts.

For the Sasso kaolin sample, specimens of the whole rock and coarser fractions still preserved structural features of the parent rock. Its pore-space distribution was inhomogeneous, and the bulk sample has a high porosity. The Sasso sample consisted of compact concentrations of well-developed plates (Figure 1B) and loosely compacted assemblages of plates and tubes (Figure 1C). Most kaolinite (and dickite) in the whole rock appeared to be well crystallized and to consist of euhedral plates in reasonably well developed stacks. Only a few coexisting kaolinitic particles were anhedral. The halloysite particles were always small (max-

https://doi.org/10.1346/CCMN.1987.0350501 Published online by Cambridge University Press

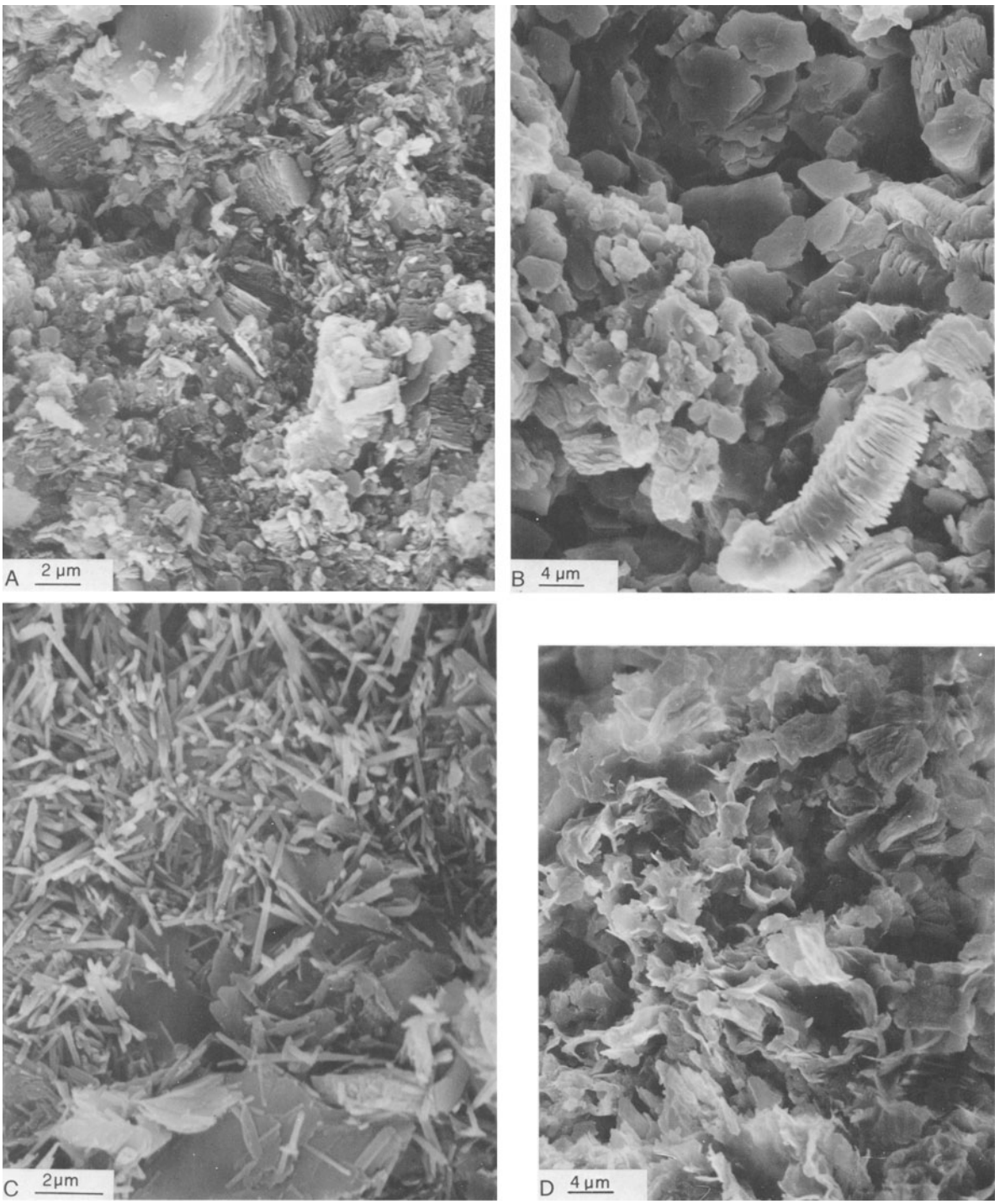

Figure 1. Scanning electron micrographs of whole rock samples: A, Georgia kaolin, showing the bimodal size distribution of large pockets of kaolinite within a matrix of finer crystals and flakes (original magnification = 4000×); B, C, D emphasize the inhomogeneity of the Sasso, Italy, hydrothermal kaolin. B, morphology of kaolinite, development of typical "books" and high porosity of the material (original magnification = 2000×). C, cluster of elongate halloysite crystals within the kaolinite plates (original magnification = 6000×). D, smectite-type or illite/smectite mixed-layer morphology (original magnification = 2000×).

https://doi.org/10.1346/CCMN.1987.0350501 Published online by Cambridge University Press

imum length <3–4 μm) and were dispersed between kaolinite (and dickite) plates or clustered in interplate pore spaces.

The presence of illite in this sample was not confirmed; the Środoń method (Środoń, 1980) gave ambiguous results. SEM-EDX showed small areas of some of the intermediate size fractions which contained only K-rich alumosilicates. Illite and mixed-layer I/S particles having curved edges and locally lying over kaolinite plates were noted in specific areas of the fracture surfaces of the whole rock (Figure 1D).

The coarser size fractions (16–8 and 8–5 μm) of both samples (Figure 2) were composed chiefly of aggregates and stacks of kaolinite plates, whereas single crystallites were present in subordinate amounts. In the Sasso sample, incompletely argillized aggregates and elongate halloysite particles were noted attached to, or interspersed among stacks and aggregates of platy crystals.

The number of aggregates in the 5–2- (Figure 3) and 2–1-μm size fractions of the Georgia sample was very small. The kaolinite plates in these and other fine size fractions were generally euhedral. The kaolinite flakes of the Sasso sample (Figure 3B) had irregular and angular edges; few elongate particles were found in this sample. Single flakes and elongate particles dominated the <1-μm size fraction and showed different morphologies with respect to components in the coarser fractions.

The kaolinite plates in the <0.5-μm size fraction of the Georgia sample were also euhedral. Their texture (Figure 4A) was secondary, induced by size fractionation and mounting of SEM stubs; original stacks of particles were apparently not preserved. Tubular elongate crystals (as in Figure 2A) were observed more frequently in the finer size fractions than in the coarser size fractions. Because EDX showed only Al and Si to be present, they must be halloysite. The fine size fractions of the Sasso sample contained abundant elongate particles, considerably longer than the e.s.d. value (Figures 4B and 4D). Kaolinite flakes had angular edges and locally occurred in stacks a few plates thick. In the finest fractions, irregularly shaped K-rich flakes were also noted that were probably mixed-layer I/S as indicated by other techniques (*vide infra*).

X-RAY POWDER DIFFRACTION RESULTS

Georgia kaolin sample

Relatively well crystallized kaolinite is dominant in the Georgia kaolin sample (Figure 5). In the whole rock and the 16–8-, 8–5-, and <0.5-μm size fractions a clear rise of the background in the small-angle region (at about 7°2θ) can be seen in the XRD patterns of both the random and oriented-slide preparations. The thermoanalytical curves of the same specimens (*vide infra*) showed a low-temperature endothermic DTA peak which is consistent with the presence of a minor amount of smectite. Fine-grained minerals such as smectite may also be trapped within the aggregates of kaolinite in the coarser size fractions.

In his investigation of Georgia kaolins, Hinckley (1961, 1965) proposed a ranking method to assess the degree of "crystal perfection" of kaolinites. His ranking is based on the variations in sharpness and relative intensity of groups of XRD peaks obtained from randomly oriented slide preparations, as marked at the base of Figures 5 and 8. The so-called Hinckley index ranks kaolinites from class 6 (most highly crystalline) to class 1 (most poorly crystalline). The kaolinite in the Georgia sample fell in class 4 in all size fractions >8–5 μm. Finer size fractions were not as highly crystalline and showed peak heights and sharpnesses typical of class 3 kaolins (Figure 5).

The kaolinite 001 peak did not change position as a function of particle size, but its symmetry (Figure 6) varied with stacking disorder, as revealed also by IR spectra (*vide infra*).

Sasso kaolin sample

In contrast to the Georgia sample, the Sasso hydrothermal kaolin showed much greater compositional and structural variations with size, as may be seen from the oriented-mount XRD patterns (Figure 7). In addition to the 001 peaks of the kaolin minerals, peaks typical of a mixed-layer mineral were observed, which were identified by glycerol and heat treatments (not reported) as a 40/60 regular I/S. The I/S was identified in the coarser size fractions, but was dominant in the finest size fractions. A few EDX analyses that showed the existence of an aluminosilicate containing potassium only, associated with the dominant kaolin minerals, suggest that illite may also have been present, together with the mixed-layer mineral, as is typical of other samples of the Sasso area (Mattias and Caneva, 1979).

Kaolinites having different degrees of crystal perfection were found to coexist with dickite in the coarser size fractions and with halloysite in the finer size fractions. Hinckley (1961) divided the 108 Georgia kaolins he studied into six classes on the basis of degree of crystal perfection. In the Sasso kaolin size fractions, effects attributable to all six classes were distinguished (Figure 8), although the XRD peak intensities of kaolinite were apparently influenced by the presence of dickite and halloysite in the coarser and finer size fractions, respectively. In the finest size fractions, no attribution to a Hinckley's class could be made, probably because the kaolin minerals' reflections were masked by the reflections of the abundant mixed-layer phase.

The XRD patterns of the random mounts of the whole rock and coarser size fractions (Figure 8) of the Sasso sample are typical of well-crystallized kaolin-group minerals. The 001 peak asymmetry (Figure 9) is

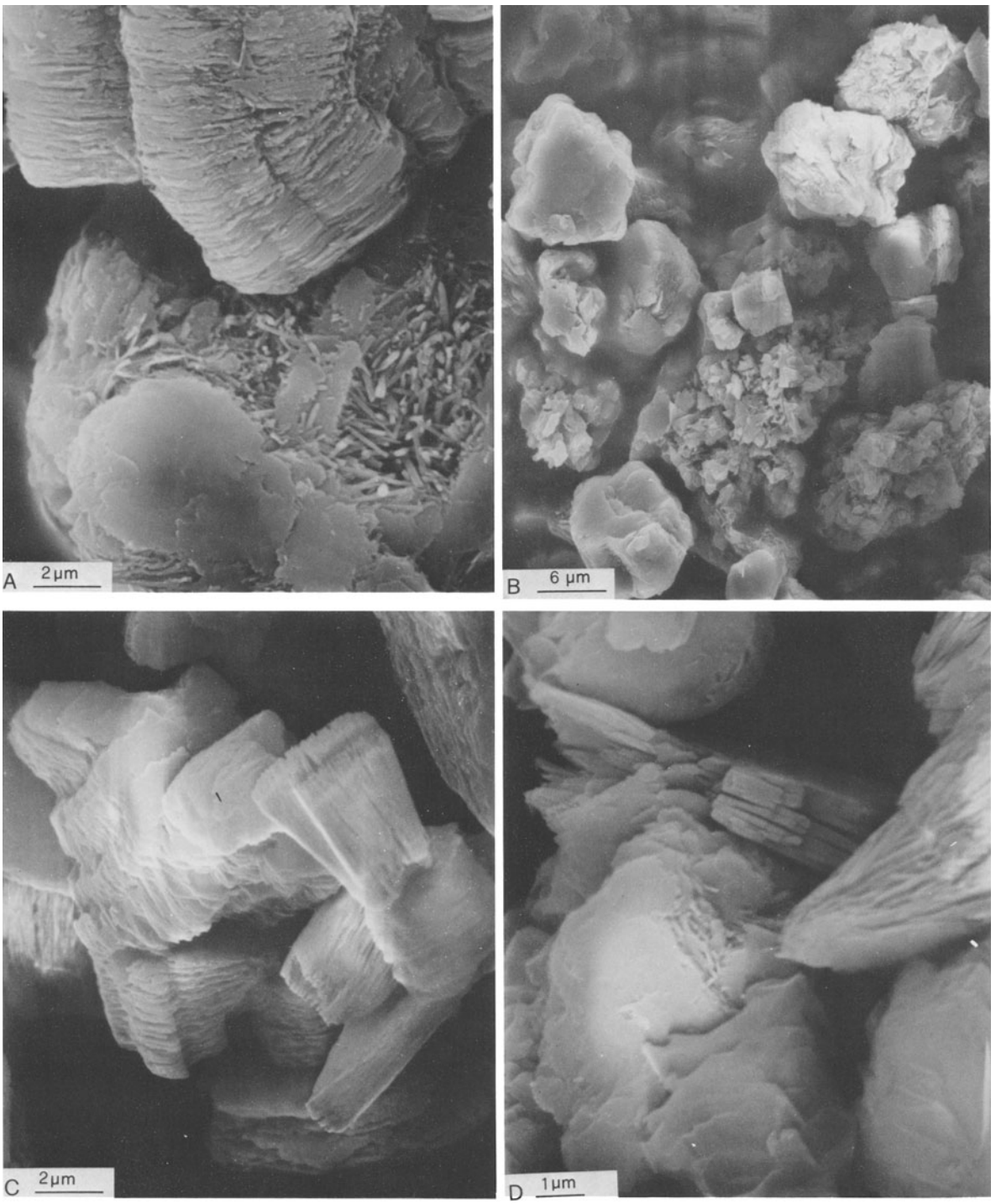

Figure 2. Scanning electron micrographs of size fractions of the Georgia and Sasso kaolins. A, Georgia kaolin, 16–8-μm fraction containing well-developed books of platy kaolinite and clusters of elongate crystals (original magnification = 6000×). B, Sasso kaolin 16–8-μm fraction containing a variety of particle morphologies (original magnification = 1500×) and possibly some incompletely altered rock fragments. C, Georgia kaolin, 8–5-μm fraction (original magnification = 6000×). D, Sasso kaolin, 8–5-μm (original magnification = 8600×). Material in C and D appears to be composed of packets of kaolinite.

https://doi.org/10.1346/CCMN.1987.0350501 Published online by Cambridge University Press

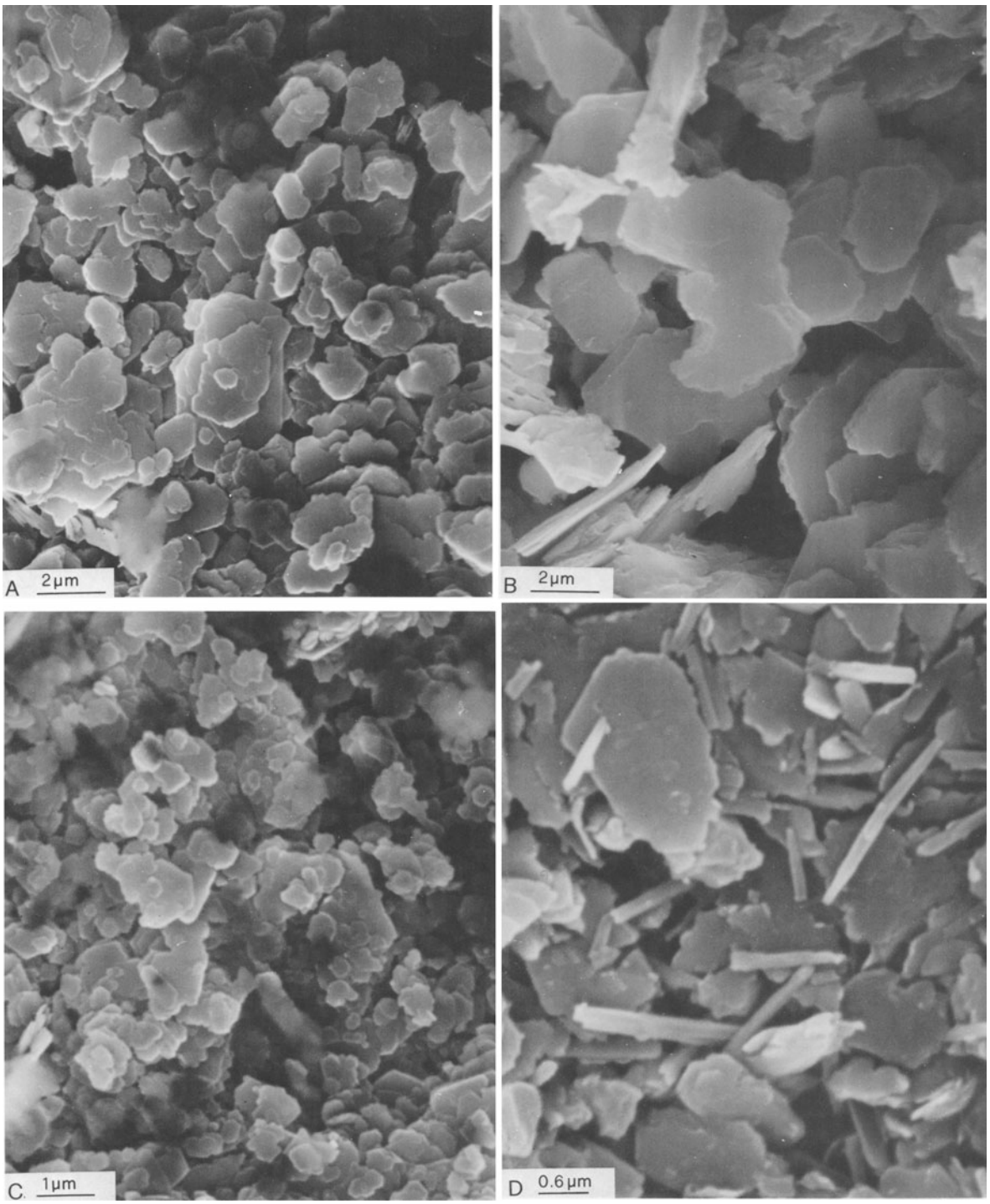

Figure 3. Scanning electron micrographs of size fractions of A, Georgia kaolin and B, Sasso kaolin 5–2-μm fractions (original magnification = 6000×) containing dominantly platy particles, although each plate may be several flakes thick. C, Georgia kaolin, 1–0.5-μm fraction (original magnification = 10,000×) is platy. D, Sasso kaolin, 1–0.5-μm fraction (original magnification = 15,000×) consists of both platy and elongate particles.

https://doi.org/10.1346/CCMN.1987.0350501 Published online by Cambridge University Press

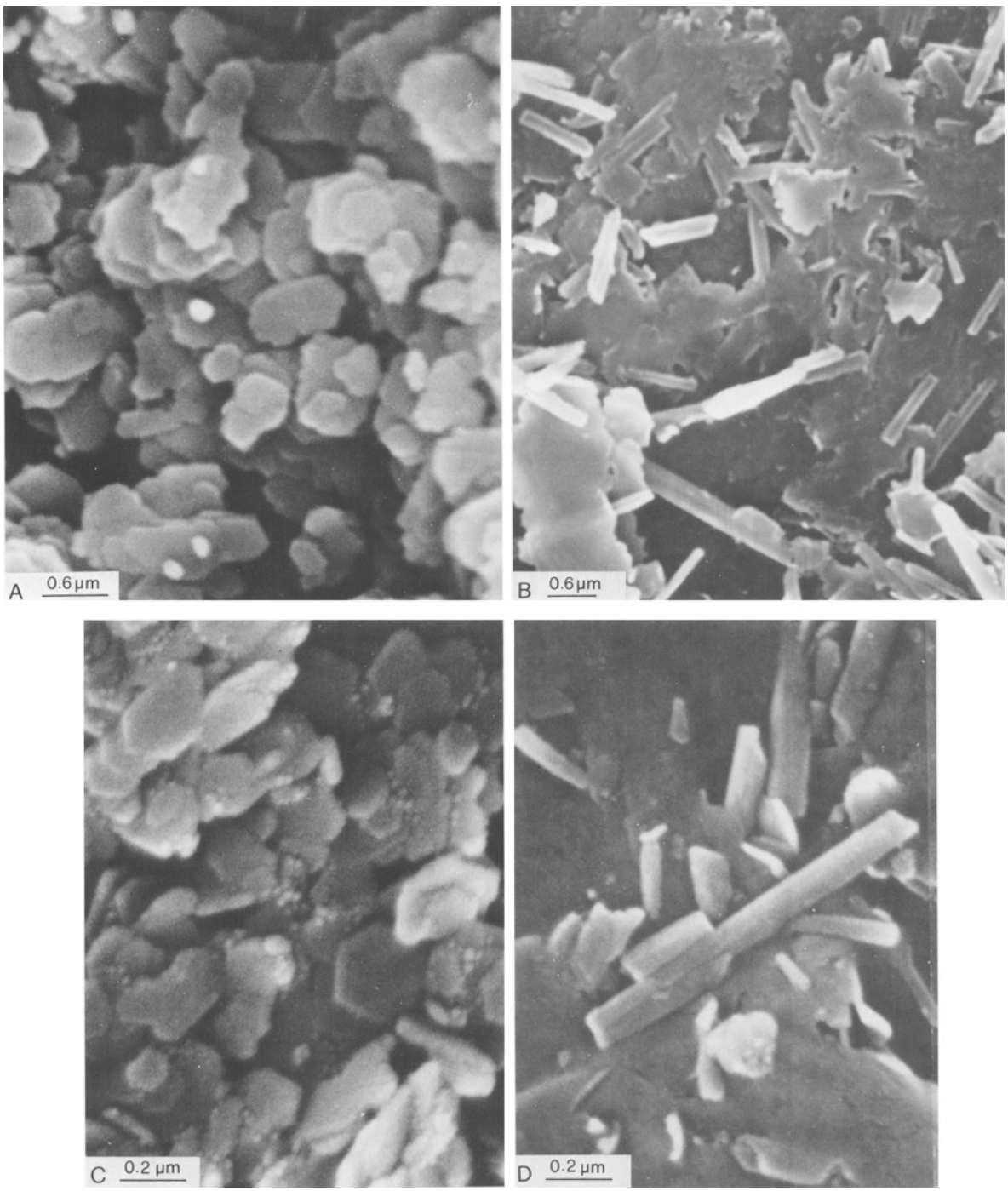

Figure 4. Scanning electron micrographs of size fractions: A, Georgia kaolin, 0.5–0.3-µm fraction containing well-developed platy crystals of kaolinite (original magnification = 20,000×). B, Sasso kaolin, 0.5–0.3-µm fraction contains fewer well-developed kaolinite crystals associated with elongate morphologies (original magnification = 15,000×). C, Georgia kaolin, <0.1-µm fraction still contains well-developed kaolinite platy crystals (original magnification = 65,000×). D, Sasso kaolin, <0.1-µm fraction contains both platy and elongate morphologies (original magnification = 65,000×).

https://doi.org/10.1346/CCMN.1987.0350501 Published online by Cambridge University Press

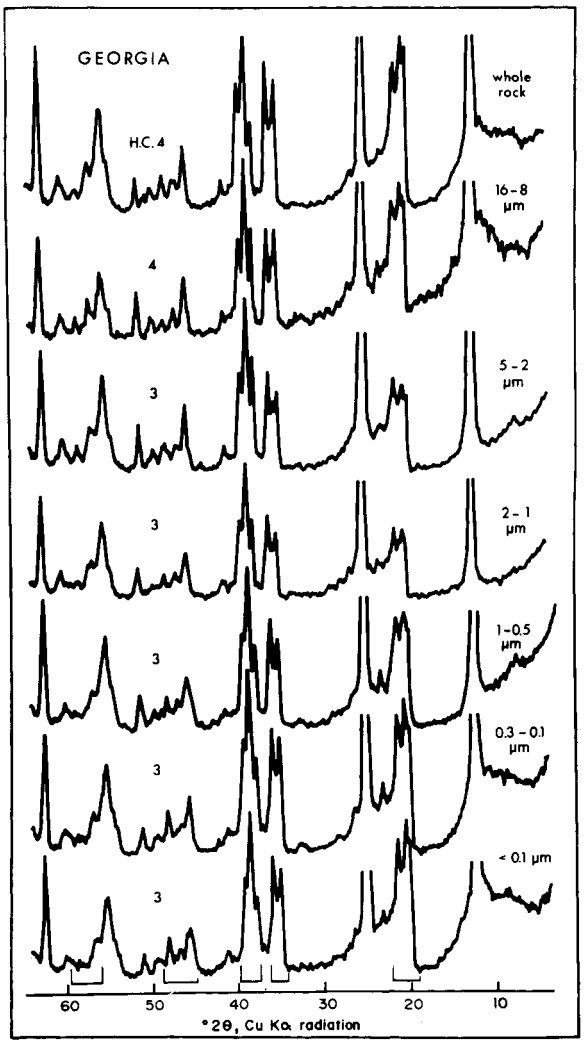

Figure 5. X-ray powder diffraction traces of the whole rock and size fractions of the Georgia kaolin. Random slides, 1°2θ/min scanning speed, Ni-filtered CuKα radiation. Crystallinity class (H.C.) according to Hinckley (1963) is indicated at left.

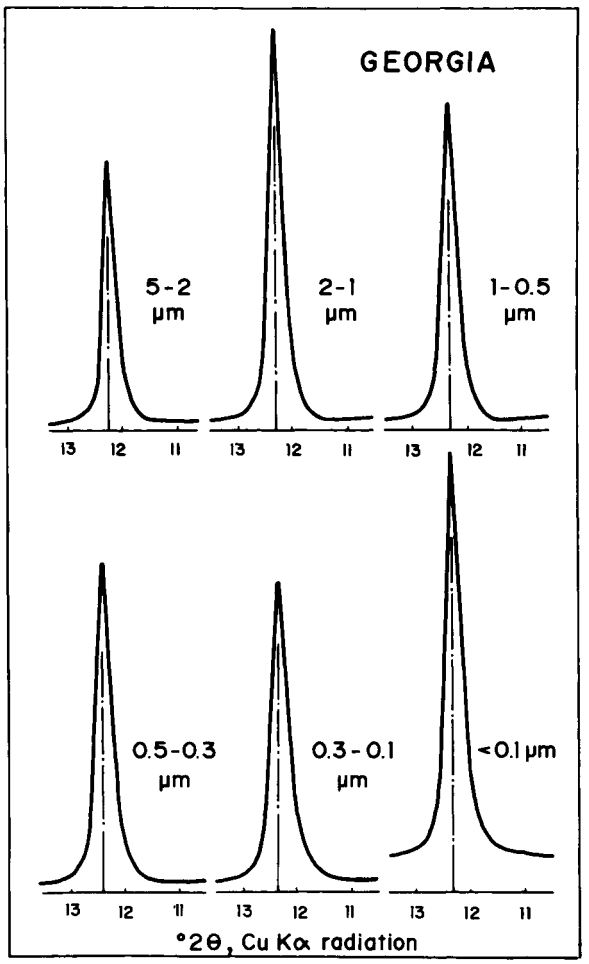

Figure 6. Variation of d(001) with particle size for the Georgia kaolin. Oriented mounts, 0.5°2θ/min scanning speed, Ni-filtered CuKα radiation.

a measure of the degree of crystalline disorder; but despite our using a range of different experimental conditions, no doublet was ever observed. The corresponding DTA curves (Figure 15) showed dehydroxylation reactions at temperatures significantly higher than for the kaolinite dehydroxylation peak at 575°C, suggesting that dickite (or nacrite) might be present. An alternative explanation for this high temperature endotherm is that it was due to large particles of highly crystalline kaolinite; however, large particles of such kaolinite can probably be discounted from the IR results (*vide infra*) and from grain-size separation of samples from the Sasso mine. These separations showed (Lombardi and Mattias, 1979) that natural mixtures of dickite and kaolinite exist, with dickite being concentrated in the coarser size fractions. Thus, the presence of the less abundant component was masked on the XRD traces, as was found by Keller and Haenni (1978) in artificial mixtures. In the finer size fractions, halloysite was abundant, as shown also by SEM and IR. In these fractions, scanned at low speed, a 001 doublet was noted, together with a sharp decrease of the height/width ratio of the peak (Figure 9). In the whole rock and coarser size fractions quartz and alunite were identified as major and minor constituents, respectively; their XRD peaks were detected down to the 1–0.5-μm size fractions.

INFRARED SPECTRA

Georgia kaolin sample

The IR spectra (Figure 10) of all particle-size fractions of the Georgia kaolin were typical of kaolinite-dominated samples (Farmer, 1974). A difference in the kaolinite crystallinity of the diverse size fractions was shown by variations in the relative intensities of the

https://doi.org/10.1346/CCMN.1987.0350501 Published online by Cambridge University Press

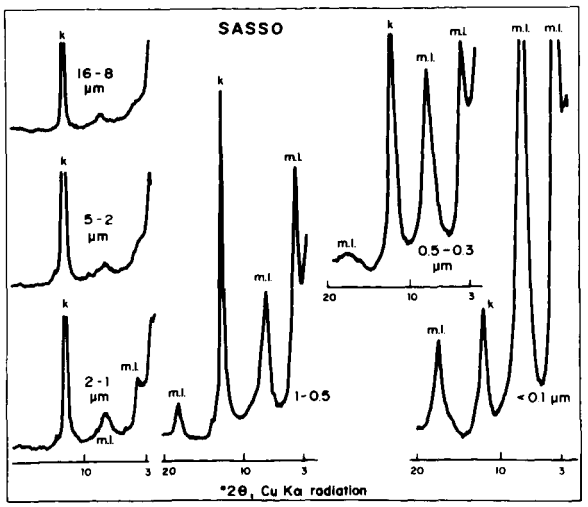

Figure 7. Small-angle X-ray powder diffraction traces of the most significative size fractions of the Sasso kaolin. Oriented mounts, 1°2θ/min scanning speed, Ni-filtered CuKα radiation. k, indicates kaolin-group minerals' peaks; m.l., peaks of mixed-layer minerals.

absorption bands in the OH-stretching region (3800–3500 cm^{-1}). In the spectra of the two coarsest fractions, the intensities of the 3620- and 3652-cm^{-1} bands relative to that at 3695 cm^{-1} was greater than what would be expected for pure, well-crystallized kaolinite (Farmer, 1974). These enhanced intensities suggest the presence of either a small amount of dickite, or, more probably, a small proportion of dickite-like stacking in the 16–8- and 8–5-μm size fractions. For all size fractions smaller than 5 μm, the spectra showed a different pattern of band intensities: only the 3652-cm^{-1} band showed enhanced intensity relative to the 3695-cm^{-1} band, all other bands showing a pattern consistent with kaolinite, i.e., the 3620-cm^{-1} band was significantly weaker than that at 3695 cm^{-1}. From a careful comparison of the relative intensities of the OH absorption bands in spectra of the three kaolinite polymorphs, kaolinite, dickite, and nacrite (Farmer, 1974), this enhancement of the 3652-cm^{-1} band probably indicates the presence of nacrite as a separate phase or of nacrite-like stacking in the kaolinite structure. The latter is more likely because the observed peak position at 3652 cm^{-1} is some 5 cm^{-1} higher than the value reported for pure nacrite (Farmer, 1974).

In the 1600–200-cm^{-1} region, the Si–O (apical) band shifted from 1096 cm^{-1} for the 8–5-μm fraction, to 1105 cm^{-1} for the 5–2-μm fraction and to 1110 cm^{-1} for the 0.5–0.3-μm fraction (Fgure 11); moreover, it was scarcely resolved from the in-plane Si–O vibration near 1118 cm^{-1}. This difference in position was an effect of decreasing particle size and arose purely from physical size (thickness mainly) of the particles in relation to the wavelength of the radiation of the absorption maximum (Farmer and Russell, 1966).

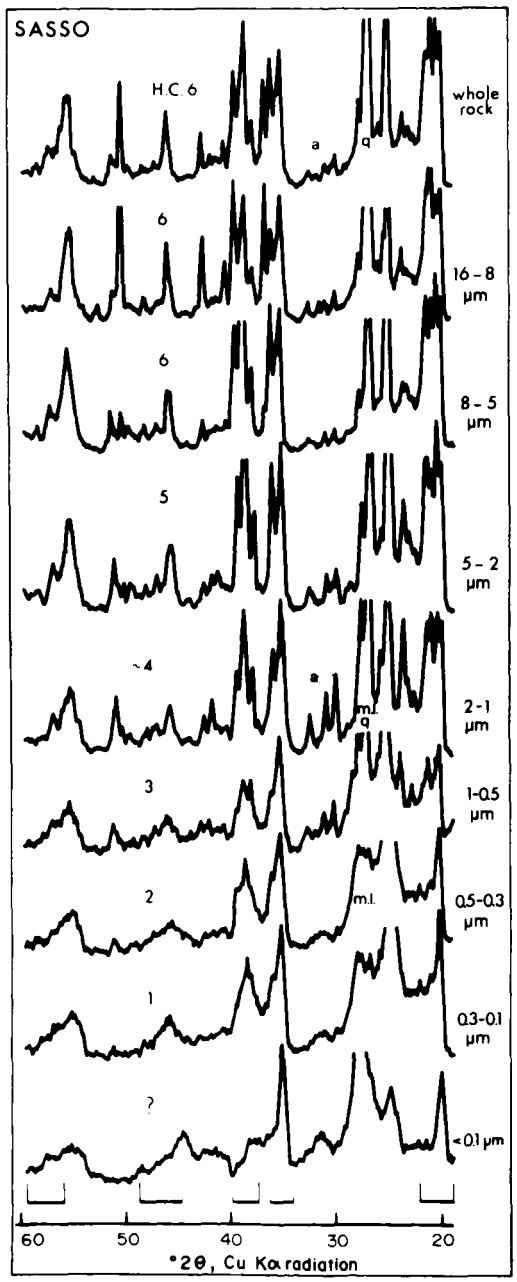

Figure 8. X-ray powder diffraction traces of the whole rock and size fractions of the Sasso kaolin. Random preparation, 1°2θ/min scanning speed, Ni-filtered CuKα radiation. Crystallinity class (H.C.) according to Hinckley (1963). a, indicates peaks of alunite; q, quartz; and m.l., mixed-layer minerals.

The 800-cm^{-1} doublet in the spectra of the coarser fractions suggests the presence of minor quartz. From the relative sharpness of the 3620-cm^{-1} kaolinite band and the absence of a marked increase in its intensity, little or no I/S was identified by IR in any of the size fractions of the Georgia sample.

https://doi.org/10.1346/CCMN.1987.0350501 Published online by Cambridge University Press

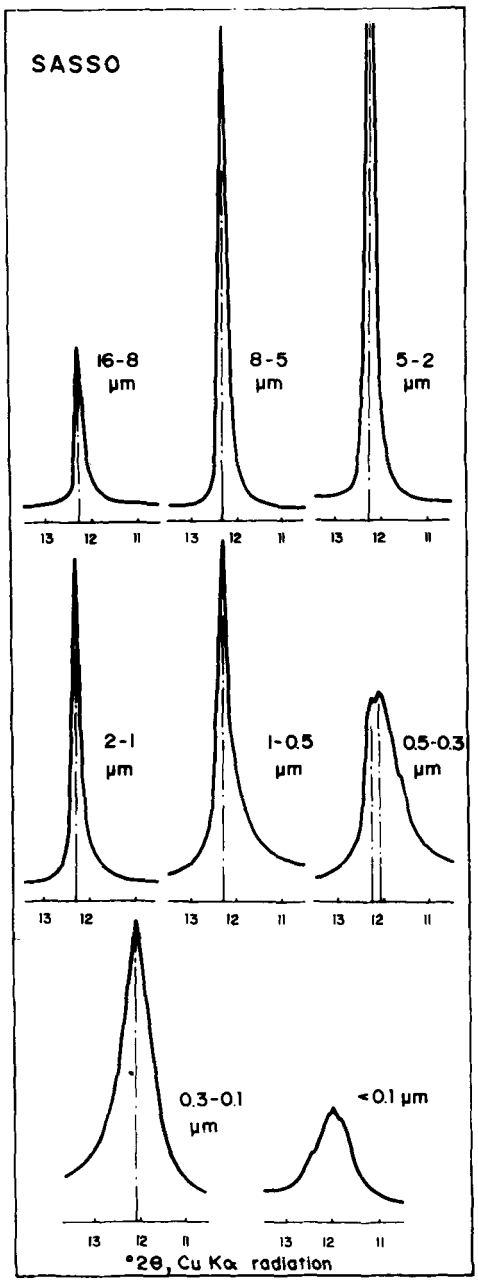

Figure 9. Variations of 001 peak shape of kaolin-group minerals with particle size. Effect of halloysite is evident in finer size fractions. Oriented mounts, 0.25°2θ/min scanning speed, Ni-filtered CuKα radiation.

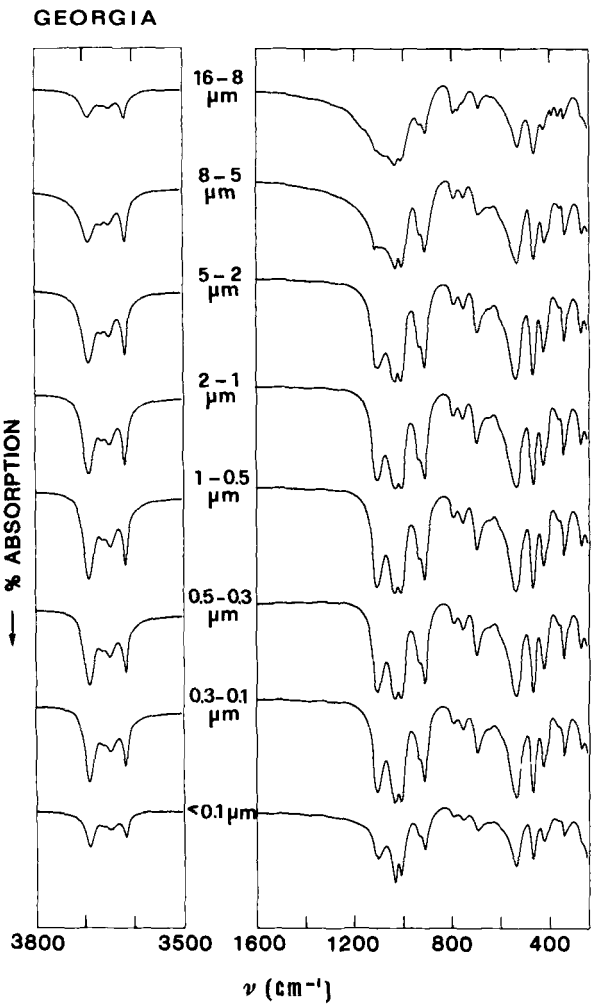

Figure 10. Infrared spectra of size fractions of the Georgia kaolin. KBr disks were heated 16 hr at 150°C.

Sasso kaolin sample

The IR spectra of the size fractions of the Sasso kaolin (Figures 12 and 13) reflected the complex mineralogy of this kaolin. As in the Georgia sample, with decreasing particle size to 1–0.5 μm, an increasing disorder was shown by an increase in dickite-like stacking (increase in intensity of the 3652-cm^{-1} band). Particle size fractions <0.5 μm, however, showed features in the OH-stretching region that were more consistent with the presence of halloysite. The general pattern of silicate absorption bands closely resembled that of Wagon Wheel (Colorado) halloysite (Van der Marel and Beutelspacher, 1976). In the finest fraction, I/S and/or illite absorption bands were dominant (broad underlying OH-stretch at 3623 cm^{-1} and band at 825 cm^{-1}). The Si–O (apical) band at 1095 cm^{-1} was significantly different from that shown by the Georgia kaolin, partly due to the <2-μm size particles in the Sasso sample being larger and somewhat thicker than those in the Georgia samples (the particles in the >2-μm fraction of the Sasso sample were thinner than those in the corresponding size fraction of the Georgia sample) and also partly due to the presence of halloysite. The halloysite and I/S contributions are more clearly seen in Figure 13. From its characteristic absorption band at 3550 cm^{-1}, halloysite was just detectable in

https://doi.org/10.1346/CCMN.1987.0350501 Published online by Cambridge University Press

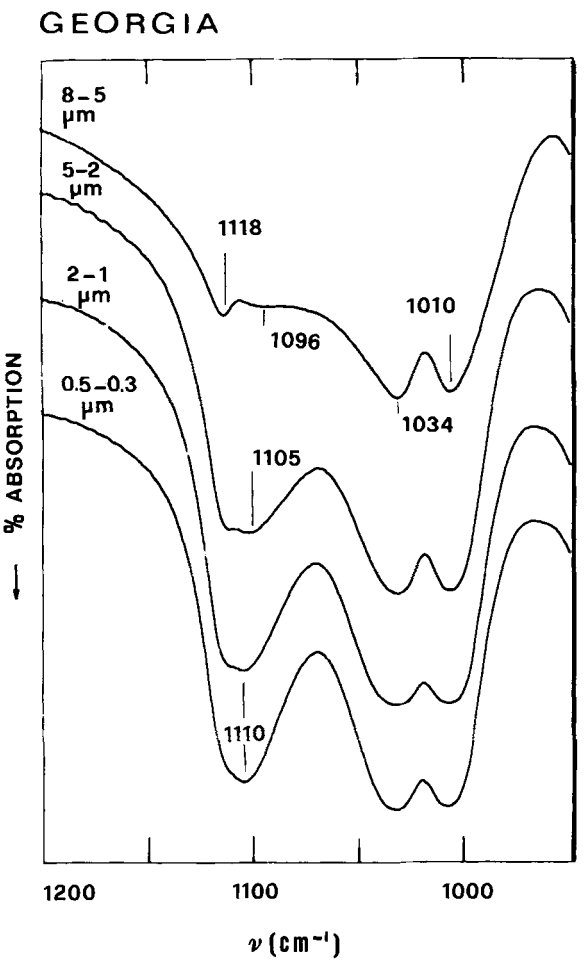

Figure 11. Infrared spectra from 950 to 1200 cm^{-1} of the Georgia kaolin. KBr disks were heated 16 hr at 150°C.

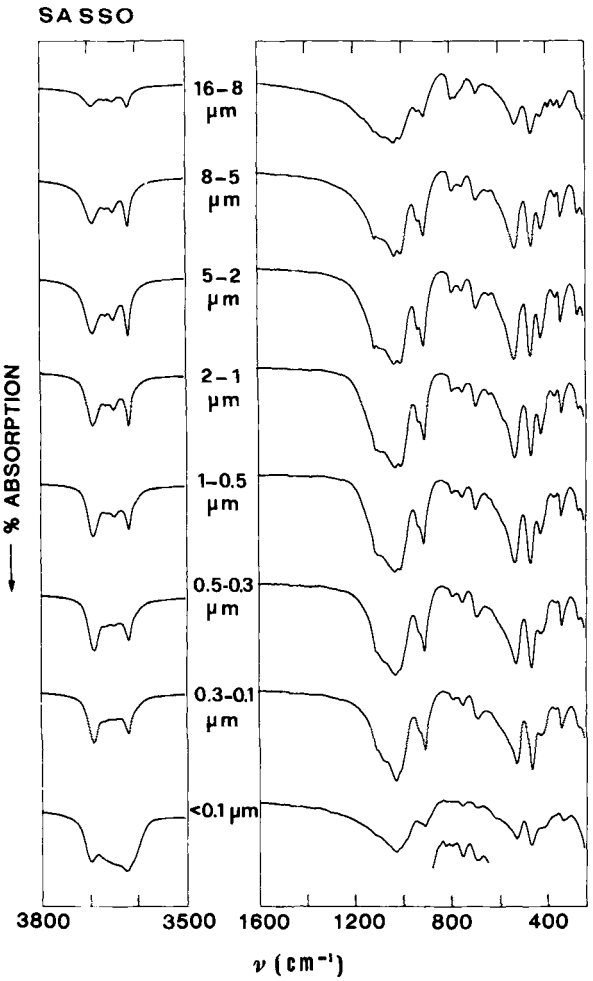

Figure 12. Infrared spectra of size fractions of the Sasso kaolin. KBr disks were heated 16 hr at 150°C.

the 1–0.5-μm size fraction and was abundant in the 0.5–0.3- and 0.3–0.1-μm size fractions. The 3550-cm^{-1} band is particularly characteristic of halloysite, possibly arising from surface OH that are hydrogen-bonded to interlayer water molecules (Kodama and Oinuma, 1963). In the samples studied here, the band disappeared after interlayer and absorbed water was removed by heating the KBr disk at 150°C (Figure 12). The spectrum of the <0.1-μm size fraction also suggests the presence of halloysite, but identification is tentative because of the dominance of I/S bands. Quartz was abundant in the 32–16-μm size fraction, significant in the 16–8-μm size fraction, and not detectable by IR in smaller size fractions.

Parker (1969) reported a method for assessing particle shape and degree of crystallinity of kaolinites by comparing the hydroxyl band intensities of samples in random orientation in KBr disks and in preferred orientation in sedimented preparations. Because of uncertainties in the degree of orientation of kaolinite particles of different sizes and shapes, the method was not used in the present investigation.

THERMOANALYTICAL RESULTS

The most significant DTA curves of the whole rock and particle-size fractions are reported in Figures 14 and 15.

Georgia kaolin sample

The DTA curves of all size fractions >0.3–0.1 μm exhibited the characteristic peaks of kaolinite. The temperature of the main endothermic dehydroxylation peaks was the same for all size fractions, although the asymmetry of the peak increased progressively with decrease of particle size. According to Bramão *et al.* (1952), higher asymmetry indexes correspond to less well crystallized forms. The differences in crystallinity among the size fractions ascertained from DTA data agree with those from IR and XRD data, which also

https://doi.org/10.1346/CCMN.1987.0350501 Published online by Cambridge University Press

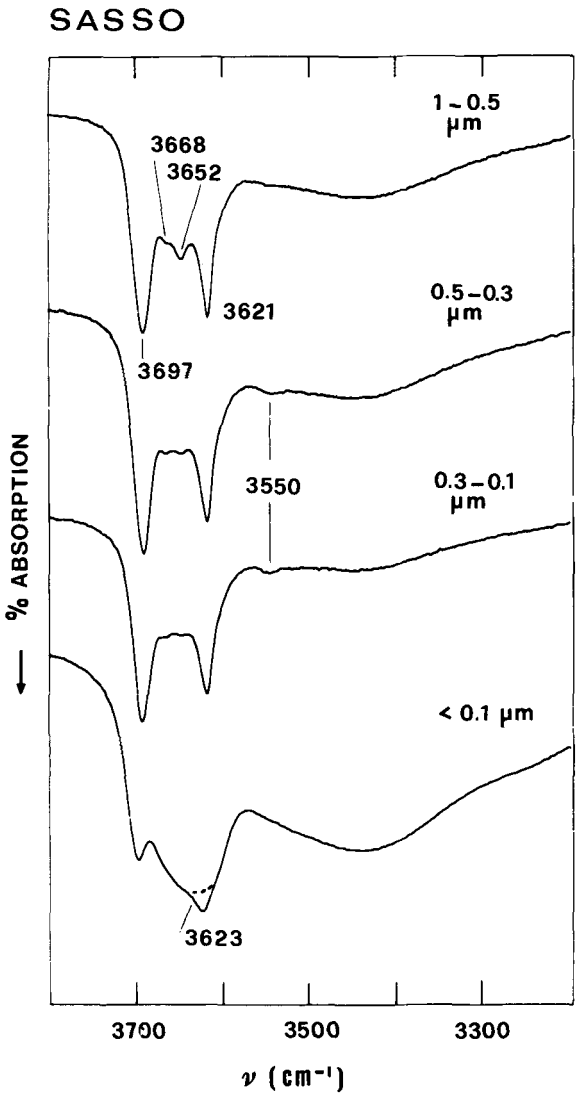

Figure 13. Infrared spectra from 3800 to 3200 cm^{-1} of the Georgia kaolin. KBr disks were not heated.

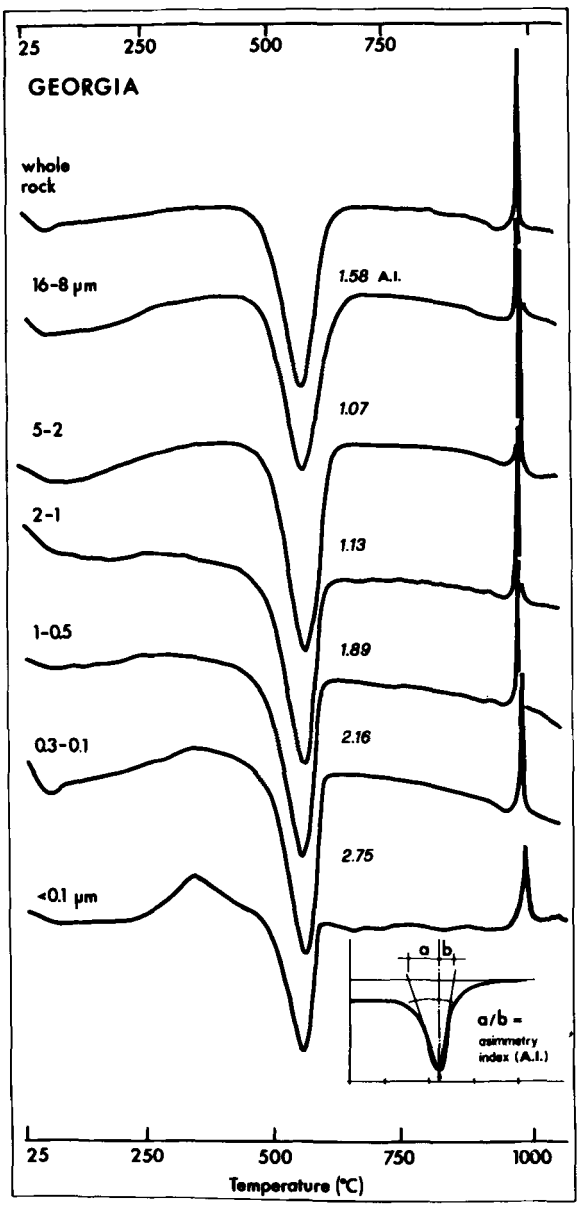

Figure 14. Differential thermal analysis curves of the whole rock and size fractions of the Georgia kaolin. Perkin-Elmer 1700 DTA; heating rate = 10°C/min; sample weight = 100 mg; static air.

show a continuous, progressive decrease in crystallinity with decreasing particle size. Taking into account the kaolinite content as calculated from TGA data (not reported), the area of the main endothermic DTA peak decreased with particle size. The exothermic peak temperature was the same for all size fractions, although its intensity decreased with decreasing particle size. A small, low-temperature, endothermic effect barely visible in the DTA pattern of the whole rock and of the 16–8-μm size fraction, but plainly evident in the 0.3–0.1- and <0.1-μm size fractions, may have arisen from a small amount of allophane. In support of this possibility, a sodium bicarbonate/dithionite treatment extracted 0.5% SiO_2 and 0.3% Al_2O_3 from the <0.1-μm size fraction. The small shoulder at about 400°C might be due to traces of organic material which has been reported as present in various Georgia kaolins. Its related weight loss is about 0.3%.

Sasso kaolin sample

In the coarsest size fractions (16–8, 8–5, and 5–2 μm) of the Sasso sample the main kaolinite endothermic peak temperature ranged from 565° to 570°C; in the finer size fractions and in the whole rock, the temperature range (Figure 15) was 545°–550°C. Holdridge and

https://doi.org/10.1346/CCMN.1987.0350501 Published online by Cambridge University Press

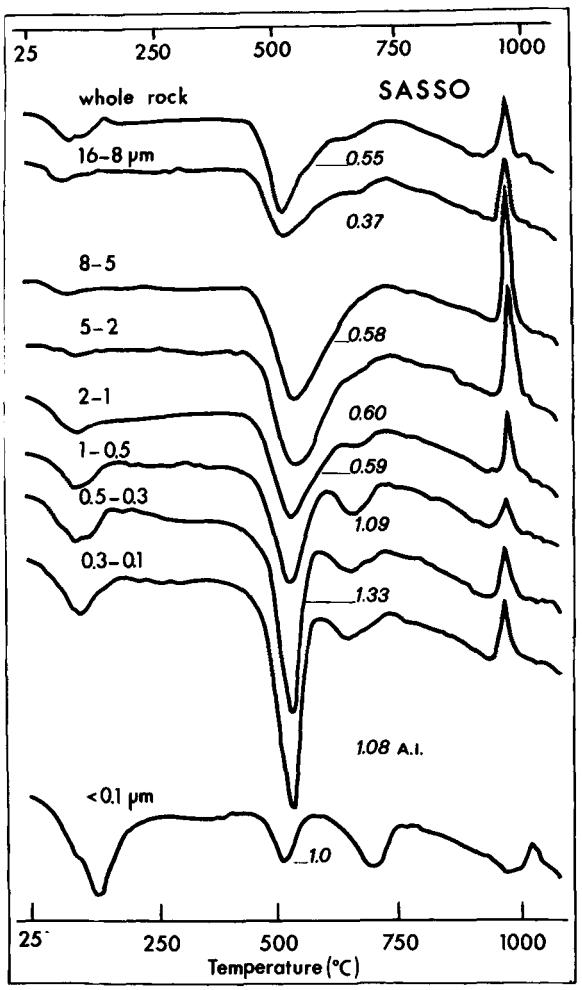

Figure 15. Differential thermal analysis curves of the whole rock and size fractions of the Sasso kaolin. Netzsch apparatus; heating rate = 10°C/min; sample weight = 100 mg; static air.

Vaughan (1957) and Smykatz-Kloss (1974a, 1974b) attributed such differences to variations in the degree of structural order and in the stacking order and style of the type indicated also by the results obtained in this work by XRD and IR analyses. For the whole rock and 16–8- and 8–5-μm size fractions, the broad peak at 680°–700°C suggests the possible presence of large particles of either well-crystallized kaolinite (Keokuk-geode type) or dickite. The presence of dickite is more likely because: (1) the XRD traces of the coarsest size fractions of the Sasso sample were close to that of dickite; Mattias and Caneva (1979) by heat and DMSO treatments of kaolins from the same area ascertained its presence; (2) in samples from the same area, a separation at the <5-μm level divided a coarser dickite-rich fraction from a finer kaolinite-rich fraction (Lombardi and Mattias, 1979); (3) a series of kaolins from the Sasso area with various kaolinite/dickite ratios was studied by Lombardi and Sheppard (1977); the XRD and DTA-TGA patterns of the kaolinite-rich members of this series were similar to those obtained for the whole rock and 16–8- and 8–5-μm size fractions in this work.

In the finest size fractions, the differences in size, peak temperature, and shape of the main dehydroxylation peak appeared to be related to the substantial amount of I/S present with respect to kaolin minerals, and to the significant amount of halloysite, as observed by SEM and indicated by IR. The increase in the halloysite content with the decrease in particle size was supported by the increase in magnitude of the low-temperature (<200°C) endotherm due to the loss of adsorbed water from size fractions between 5–2 μm and 0.3–0.1 μm. The DTA pattern of the <0.1-μm fraction was markedly different due to the dominance of non-kaolin clay minerals. The peak temperature and morphology of the high-temperature exothermic peak of the kaolin-group minerals were similar for all size fractions, except the finest. The height and area were roughly proportional to the kaolin-group mineral content of the sample as calculated from the TGA curves (not reported). In all DTA curves a small endothermic effect immediately preceded the 980°–985°C exothermic peak. According to Holdridge and Vaughan (1957 and literature cited therein), this peak is typical of well-crystallized kaolinite. SEM shows that even in the smaller size fractions, kaolinite crystals are euhedral, despite the fact that XRD traces showed clear evidence of a marked variation of crystallinity with particle size.

In the <0.1-μm fraction, the thermal effects were mainly those of I/S, which predominated over the kaolin-group minerals.

MINERALOGICAL COMPOSITION OF THE TWO KAOLIN SAMPLES

The mineralogical composition of the Georgia and Sasso samples, as derived from the entire set of analyses of both whole rocks and particle size fractions, are summarized as follows. The Georgia sample consists of dominant, well-crystallized, fine-grained kaolinite and minor quantities of elongate halloysite-like particles and smectite. Traces of organic material and minor amounts of quartz are present in the coarser fractions, and minor amounts of noncrystalline components appear to be present in the finest fractions. The Sasso sample consists of dominant kaolinite of various grain sizes and crystallinities, dickite in the coarser and halloysite in the finer fractions, regular mixed-layer I/S in the finer fractions (becoming dominant in the finest), and abundant quartz and traces of alunite in the whole rock and coarser fractions. The results of a semi-quantitative mineralogical analysis based on XRD and thermoanalytical data of this sample are given in Figure 16.

https://doi.org/10.1346/CCMN.1987.0350501 Published online by Cambridge University Press

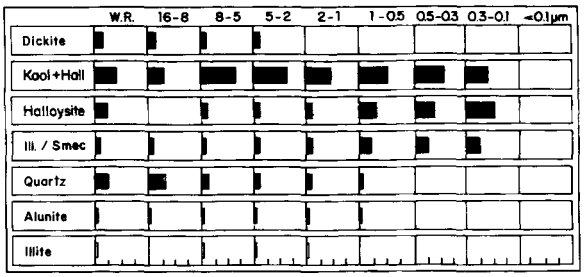

Figure 16. Semi-quantitative assessment of the mineralogical composition in the various size fractions of the Sasso kaolin, as derived from X-ray powder diffraction and thermoanalytical data. Kaol, kaolinite; Hall, halloysite; Ill, illite; Smec, smectite. Tic marks on abscissa correspond to 25%, 50%, and 75%.

DISCUSSION

This work demonstrates that more than one analytical technique should be used to acquire the compositional and structural picture of the constituents of a clay sample. As shown by the data presented here, size is associated with much more compositional and structural changes in the hydrothermal Sasso kaolin sample than in the sedimentary Georgia kaolin sample. If only the whole rock or large-particle size fractions are analyzed, constituents which are abundant in smaller particle size fractions may not be detected if only one analytical technique is used. For example, the <0.1-μm size fraction of the Sasso kaolin sample displayed mineralogical properties which departed significantly from those of the whole rock sample. As a consequence, analysis of the whole rock permitted only partial insight into its constituents. Moreover, XRD, IR, and DTA patterns are often dominated by species which are most sensitively detected by these techniques but which are not necessarily the most abundant. For example, the XRD pattern of well-crystallized kaolinite disguises that of less well crystallized kaolinite; many of the DTA peaks of the illitic component are in part overlapped by those of the kaolin minerals.

In the Georgia kaolin sample the crystallinity of the dominant kaolinite decreased slightly with decreasing particle size and exhibited moderate changes in type of stacking. Similar size-induced changes in crystallinity were reported by Hassanipak and Eslinger (1985) in the 2–1-, 1–0.5- and <0.5-μm Georgia kaolin size fractions from both Cretaceous and Tertiary deposits. Based on δO^{18} values which, for a given sample, decreased with increasing crystallinity and size, the above authors inferred "that post-sedimentation recrystallization resulted in larger than average crystallite sizes having higher C.I. (crystallinity index) values and that this recrystallization occurred in a warmer environment and/or in the presence of ground waters with a lower δO^{18} relative to that in which the original kaolin crystallized."

Halloysite did not constitute a major phase in the Georgia kaolin sample. In the 16–8-μm size fraction of the sample analyzed, a small cluster of elongate particles (halloysite?) was identified; however, the amount of such particles was so small that they could not be detected after clay dispersion. The amount of noncrystalline material in the <0.1-μm fraction of the Georgia kaolin sample, determined by chemical extraction, proved to be minimal (<1%). Nonetheless, W. F. Bundy and H. H. Murray (Georgia Kaolin Company, unpublished work, referenced in Grim, 1972) stated that even tiny amounts of noncrystalline material undetected by electron micrographs can influence dispersion, viscosity, and other properties of the Georgia kaolin.

The complex assemblages of the size fractions of the Sasso kaolin appear to be the product of a multiphase hydrothermal process ranging over a broad spectrum of temperatures and fluid chemistries. The well-crystallized dominant kaolinite and dickite are the result of the main stage of hydrothermal alteration of the local rhyolites and quartz latites. O/H isotope data (Lombardi and Sheppard, 1977) indicate that such alteration occurred at temperatures <80°C. Such alteration processes are still active today; low-temperature CO_2- and halogen-rich fluids percolating through the altered volcanics can still be observed in the field. This fact suggests that the dickite → well-crystallized kaolinite → less well crystallized kaolinite sequence in the various size fractions may be mainly temperature-dependent.

Halloysite is abundant in the fine fractions of the Sasso kaolin where both 10-Å and 7-Å halloysites have been detected (Lombardi and Mattias, 1979). It is randomly scattered throughout the sample in clusters either between or on top of the kaolin plates. Halloysite is more abundant in alunite-rich samples from alteration areas where sulfur isotope data point to recent supergene processes as responsible for most of the alunite (Field and Lombardi, 1972). This finding supports the proposition that at least part of the halloysite was formed during a late stage of development of this kaolin. In the Sasso kaolin, I/S is present in all the fractions and dominates the very fine ones. It is never the sole component in any particle size fraction, but minor amounts of it, combined with illite, have been encountered in most of the samples from the Sasso and genetically similar Tolfa areas (Lombardi and Mattias, 1979). The I/S must have formed in an alteration environment less acidic than that giving rise to the kaolin minerals. I/S (and illite) thus likely represents a late stage in which waters percolating through altered porous volcanics in an environment rich in noncrystalline silica were conducive to the formation of the 2:1 clay minerals.

Despite the fact that only two kaolin samples were examined in the present study, it indicates that greater stress should be placed on examining the compositional homogeneity of different size fractions of a given

clay sample. Many clays defined as "homogeneous" may only be such because of scanty data on their mineralogy. This study has shown that size fractions may involve an enrichment in a given phase that could substantially influence the industrial processing of kaolin. As a result, clay processing should incorporate provisions for detecting possible enrichment or depletion in specific constituents upon size fractionation.

ACKNOWLEDGMENTS

Part of this work was carried out at the Geology Department of Indiana University, where one of the authors (G.L.) was a visiting professor. Helpful discussions with H. H. Murray are gratefully acknowledged. The authors thank F. De Gennaro of the University of Naples and A. Magri of the University of Rome for use of their thermoanalytical apparatus and M. Tait and A. R. Fraser of the Macaulay Institute for Soil Research of Aberdeen for TEM work and analysis of noncrystalline material, respectively. Scanning electron micrography was supported by NSF Grant EAR 8110592 to W.D.K.

REFERENCES

Bramão, L., Cady, J. G., Hendricks, S. B., and Swerdlow, M. (1952) Characterization of kaolin minerals: *Soil Sci.* **73,** 273–287.

Brindley, G. W., de Souza Santos, P., and de Souza Santos, H. L. (1963) Mineralogical studies of kaolinite-halloysite clays: Part I. Identification problems: *Amer. Mineral.* **48,** 897–910.

Byström-Asklund, A. M. (1966) Sample cups and a technique for sideward packing of X-ray diffractometer specimens: *Amer. Mineral.* **51,** 1233–1237.

Farmer, V. C. (1974) The layer silicates: in *The Infrared Spectra of Minerals,* V. C. Farmer, ed., Mineralogical Society, London, 331–363.

Farmer, V. C. and Russell, J. D. (1966) Effects of particle size and structure on the vibrational frequencies of layer silicates: *Spectrochim. Acta* **22,** 389–398.

Field, C. and Lombardi, G. (1972) Sulfur isotopic evidence for the supergene origin of alunite deposits, Tolfa district, Italy: *Miner. Deposita* **7,** 113–125.

Galan, E., Mattias, P. P., and Galvan, J. (1977) Correlacion entre cristalinidad, tamaño, genesis y edad de algunas caolinitas españolas: in *Proc. 8th Int. Kaolin Symp. and Meet. on Alunite, Madrid-Rome, 1977,* E. Galan, ed., Ministerio de Industria y Energia, Madrid, 8 pp.

Grim, R. E. (1972) Technical properties and application of clays and clay minerals: in *Proc. Int. Clay Conf., Madrid, 1972,* J. M. Serratosa, ed., Consejo Superior de Investigaciones Cientificas CSIC, Madrid, 719–721.

Hassanipak, A. A. and Eslinger, E. (1985) Mineralogy, crystallinity, δO18/O16, and D/H of Georgia kaolins: *Clays & Clay Minerals* **33,** 99–106.

Hinckley, D. N. (1961) Mineralogical and chemical variations in the kaolin deposits of the Coastal Plain of Georgia and South Carolina: Ph.D. thesis, the Pennsylvania State University, University Park, Pennsylvania, 206 pp.

Hinckley, D. N. (1963) Variability in "crystallinity" values among the kaolin deposits of the Coastal Plain of Georgia and South Carolina: in *Clays and Clay Minerals, Proc. 11th Natl. Conf., Ottawa, Ontario, Canada, 1962,* W. F. Bradley, ed., Pergamon Press, New York, 229–235.

Hinckley, D. N. (1965) Mineralogical and chemical variations in the kaolin deposits of the Coastal Plain of Georgia and South Carolina: *Amer. Mineral.* **50,** 1865–1883.

Holdridge, D. A. and Vaughan, F. (1957) The kaolin minerals (kandites): in *The Differential Thermal Analysis of Clays,* R. C. Mackenzie, ed., Mineralogical Society, London, 98–139.

Hurst, V. J., ed. (1979) *Field Conference on Kaolin, Bauxite and Fuller's Earth:* Clay Minerals Society Annual Meeting, Macon, Georgia, 1979, 107 pp.

Keller, W. D. (1977) Scan electron micrographs of kaolins collected from diverse environments of origin—IV. Georgia kaolin and kaolinizing source rocks: *Clays & Clay Minerals* **25,** 311–345.

Keller, W. D. and Haenni, R. P. (1978) Effects of micro-sized mixtures of clay minerals on properties of kaolinites: *Clays & Clay Minerals* **26,** 384–396.

Keller, W. D., Galan, E., and Mattias, P. P. (1977) Scan electron micrographs of clays from field-trip localities of the VIII International Kaolin Symposium, Spain and Italy, 1977: in *Proc. 8th Int. Kaolin Symp. and Meet. on Alunite, Madrid-Rome, 1977,* E. Galan, ed., Ministerio de Industria y Energia, Madrid, 10 pp.

Kocsardy, E. and Heydemann, A. (1980) Characterization of kaolin minerals of different origin: *Acta Miner. Petr. Saged Suppl.* **24,** 91–99.

Kodama, H. and Oinuma, K. (1963) Identification of kaolin minerals in the presence of chlorite by X-ray diffraction and infrared absorption spectra: in *Clay and Clay Minerals, Proc. 11th Natl. Conf., Ottawa, Ontario, 1962,* Ada Swineford, ed., Pergamon Press, New York, 236–249.

Lombardi, G. and Mattias, P. (1979) Petrology and mineralogy of the kaolin and alunite mineralizations of Latium (Italy): *Geol. Romana* **18,** 157–214.

Lombardi, G. and Sheppard, S. M. F. (1977) Petrographic and isotopic studies of the altered acid volcanics of the Tolfa-Cerite area, Italy. The genesis of the clays: *Clay Miner.* **12,** 147–162.

Mattias, P. and Caneva, C. (1979) Mineralogia del giacimento di caolino di M. Sughereto (Santa Severa, Roma): *Rend. Soc. It. Miner. Petr.* **35,** 721–753.

Murray, H. H. (1976) The Georgia sedimentary kaolins: in *Proc. 7th Symp. Genesis of Kaolin, Int. Geol. Correlation Program, Committee on Correlation of Age and Genesis of Kaolin, Tokyo, Japan, 1976,* H. Minato, ed., 114–125.

Olivier, J. P. and Sennett, P. (1972) Particle size-shape relationships in Georgia sedimentary kaolins—II: in *1972 Int. Clay Conf. Kaolin Symp. Proc.,* J. M. Serratosa, ed., Consejo Sup. de Investigaciones Cientificas, CSIC, Madrid, 171–173.

Parker, T. W. (1969) Classification of kaolinites by infrared spectroscopy: *Clay Miner.* **8,** 135–141.

Smykatz-Kloss, W. (1974a) The determination of the degree of (dis-)order of kaolinites by means of DTA: *Chemie der Erde* **33,** 358–366.

Smykatz-Kloss, W. (1974b) *Differential Thermal Analysis. Applications and Results in Mineralogy:* Springer-Verlag, Berlin, 188 pp.

Środoń, J. (1980) Precise identification of illite/smectite interstratification by X-ray powder diffraction: *Clays & Clay Minerals* **28,** 401–411.

Tanner, C. B. and Jackson, M. L. (1947) Nomographs of sedimentation times for soil particles under gravity or centrifugal acceleration: *Soil Sci. Soc. Amer. Proc.* **11,** 60–65.

Van der Marel, H. W. and Beutelspacher, H. (1976) *Atlas of Infrared Spectroscopy of Clay Minerals and Their Admixtures:* Elsevier, Amsterdam, 396 pp.

(Received 27 August 1986; accepted 15 March 1987; Ms. 1606)